Attribution of climate change and human activities to vegetation NPP dynamics in southwest China: A zonal comparison between Karst and Non-Karst areas

Huijun Xie[1,2], Qingjiang Du[3*], Xun Jiang[2,4]

[1] Key Laboratory of the Three Gorges Reservoir Region's Eco-Environment, Ministry of Education, College of Environment and Ecology, Chongqing University, Chongqing 400045, China.

[2] Nanjiang Hydrogeology and Engineering Geology Team, Chongqing Bureau of Geology and Minerals Exploration, Chongqing 401121, China.

[3] No. 208 Hydrogeology and Engineering Geology Team, Chongqing Bureau of Geology and Minerals Exploration (Chongqing Reconnaissance and Design Academy of Geological Disaster Prevention and Treatment Engineering), Chongqing 400700, China.

[4] College of Civil Engineering, Chongqing University, Chongqing 400045, China.

*Corresponding Author e-mail: dqj.csedu@outlook.com

Received: 2 November 2025 / Accepted: 19 October 2026

Abstract. To elucidate the geological background-dependent responses of vegetation net primary productivity (NPP) to climate change and human activities in Southwest China, this study integrated multi-source datasets from 2001 to 2019, including NPP, land use, temperature, precipitation, relative humidity, and sunshine duration. Trend analysis and partial derivative analysis were employed to investigate the spatiotemporal dynamics of NPP in karst and non-karst areas and to quantify the respective effects of climate change and human activities. The results showed that: (1) NPP exhibited an overall fluctuating upward trend across the study area, with a rate of increase of 3.35 $gC \cdot m^{-2} \cdot yr^{-1}$. The mean NPP and growth rate were slightly higher in karst areas than in non-karst areas. However, the proportion of areas showing significant increases was lower, and the risk of localized degradation was higher, in karst areas. (2) From 2001 to 2019, land-use transition patterns in both karst and non-karst areas of Southwest China were dominated by shrubland-to-forestland and cropland-to-shrubland transitions. NPP changes differed between the two areas under the same land-use transitions. In areas transitioning from cropland to forestland, the NPP increase was lower in karst areas (135.57 $gC \cdot m^{-2}$) than in non-karst areas (188.58 $gC \cdot m^{-2}$), whereas NPP increases in areas transitioning from grassland to forestland or shrubland were greater in karst areas. In addition, forestland-to-shrubland and shrubland-to-cropland transition areas showed opposite NPP change patterns between karst and non-karst areas. (3) The residual-proxy estimate of the human activity contribution to NPP change was 3.09 $gC\ m^{-2}\ yr^{-1}$, approximately three times the climatic contribution (1.03 $gC\ m^{-2}\ yr^{-1}$) in Southwest China. The estimated human activity contribution was higher in karst areas than in non-karst areas, whereas the

climatic contribution was more pronounced in non-karst areas, with precipitation contributing the most. (4) In karst areas, NPP increases were mainly driven by human activities and the combined effects of climate and human activities (accounting for 54% of the area), whereas climate-driven NPP increases were more extensive in non-karst areas (accounting for 33.03% of the area). Overall, the combined effects of climate and human activities exerted a greater influence on NPP changes. These findings highlight the heterogeneous responses of vegetation productivity to climate and human activities under contrasting geological backgrounds and provide a scientific basis for differentiated ecological restoration and carbon sink management in Southwest China.

Keywords: climate change; human activities; contribution analysis; Karst ecosystem; land use change

1. Introduction

Net primary productivity (NPP) is defined as the amount of organic matter accumulated by green vegetation per unit area and unit time, representing the residual carbon fixed after subtracting autotrophic respiration (RA) from gross primary productivity (GPP) (Guo et al., 2020; Ewuketu et al., 2020). NPP serves as an effective indicator for assessing the carbon budget of terrestrial ecosystems (Zhong et al., 2021; Guan et al., 2019) and reflects ecosystem health and productivity (Yang et al., 2021; Wu et al., 2020; Zhao et al., 2020; Erb et al., 2016). Climate change and human activities are two critical factors influencing vegetation dynamics (Zheng et al., 2019). Global warming and intensifying human activities have further altered the spatiotemporal patterns of vegetation NPP (Ge et al., 2021; Liu et al., 2018).

NPP is highly sensitive to climate change (Wang et al., 2021; Wu et al., 2021). Climate warming can enhance the rates of vegetation photosynthesis and plant growth, thereby promoting NPP accumulation (Teng et al., 2020). However, precipitation may exert an even stronger influence on NPP in some areas (Wang et al., 2019). Overall, the effects of climate on NPP exhibit pronounced spatial heterogeneity. Climatic conditions promote vegetation growth across the mid- and high-latitude regions of the Northern Hemisphere (Nemani et al., 2003), whereas they constrain vegetation growth in some other areas (Wu et al., 2020; Prestele et al., 2017). The responses of NPP to climate in China also exhibit substantial spatiotemporal variability (Hong et al., 2021).

For example, NPP in the western Qiangtang Plateau is primarily limited by precipitation, whereas that in the eastern part is more strongly constrained by evapotranspiration or temperature (Zhou et al., 2021). At the monthly scale, NPP in the mountainous areas of Southwest China is more strongly influenced by temperature than by precipitation (Wang et al., 2021), whereas NPP variations across most of Inner Mongolia are jointly driven by temperature and precipitation (Liu et al., 2021). In addition to climatic factors, human activities are also important drivers of NPP dynamics. Land-use change represents one of the most direct manifestations of the impacts of human activities on the natural environment (Yang et al., 2021; Taelman et al., 2016) and influences the carbon cycle by altering terrestrial carbon stocks and fluxes (Wu et al., 2014). Research indicates that environmentally beneficial human activities can promote vegetation carbon sequestration. Since 2000, China has implemented a series of ecological conservation measures, including afforestation, forest protection, and the conversion of cropland to forestland, which have increased vegetation cover (Lv et al., 2018). Chen et al. (2020) showed that, in the context of ecological restoration projects, the expansion of planted forests in China from 1982 to 2014 promoted increases in forest leaf area index (LAI) and NPP [18]. However, detrimental human activities, such as grazing, forest logging, and urbanization, may reduce ecosystem productivity (Teng et al., 2020). Yan et al. (2021) found that rapid urbanization encroached upon cropland, resulting in NPP losses.

The karst areas of Southwest China represent one of the largest terrestrial carbon sink areas in China (Xiao et al., 2024) and play an important role in soil and water conservation, climate regulation, and carbon sequestration (Wu et al., 2020). Compared with non-karst areas, karst areas have shallow soil layers and a high degree of rock exposure (Hong et al., 2021; Lv et al., 2018). In addition, the development of bedrock fractures leads to rapid leakage of surface water, making vegetation in these areas highly sensitive to changes in precipitation (Shuai et al., 2025). At the same time, karst areas have poor water-retention capacity, and increasing temperatures can significantly increase evapotranspiration, which may further affect the accumulation of photosynthetic products (Luo et al., 2024; Liu et al., 2016). In addition, unsustainable

land-use practices, such as cultivation and deforestation, in karst areas can easily exacerbate soil erosion, thereby reducing NPP. Although ecological restoration projects, such as the conversion of cropland to forest and rocky desertification control, can improve vegetation carbon sequestration efficiency (Zhou et al., 2025; Du et al., 2024), their recovery rate and potential for carbon sink enhancement may differ from those in non-karst areas because of soil infertility and water deficits in karst areas. Therefore, investigating differences in vegetation productivity between karst and non-karst areas is important for understanding the mechanisms driving vegetation carbon sinks under different geological settings.

Most previous studies have focused on the combined effects of climate change and human activities, without explicitly quantifying their respective contributions to NPP. Although some studies have attempted to separate these effects, systematic comparisons between karst and non-karst areas remain limited. Therefore, based on multi-source remote sensing data and ground-based observations, this study employed trend analysis, a land-use transition matrix, and partial derivative analysis to investigate the spatiotemporal dynamics of NPP and the respective effects of climate and human activities in karst and non-karst areas. Based on these analyses, the following hypotheses were proposed: (1) NPP exhibits an overall increasing trend in the study area, but the risk of NPP degradation may be higher in karst areas than in non-karst areas. (2) NPP dynamics in areas undergoing the same land-use transitions may differ between karst and non-karst areas because of differences in geological background. (3) The impact of human activities on NPP may be greater in karst areas than in non-karst areas, whereas the influence of climatic factors on NPP may be weaker in karst areas than in non-karst areas.

2. Materials and Methods

2.1. Study area

The study area mainly encompasses four provincial-level administrative regions—Sichuan, Chongqing, Yunnan, and Guizhou. It is located in the transitional zone between the first and second topographic steps of China. It covers a total area of

1.13×10^6 km², accounting for approximately 11.77% of China's land area. The terrain includes plateaus, mountains, hills, and plains, with elevations generally decreasing from west to east and ranging from 50 to 7100 m (Figure 1a). The region exhibits diverse landforms, with karst landforms accounting for approximately 37.35% of the total area. The bedrock is dominated by carbonate rocks, primarily limestone and dolomite. Although groundwater resources are abundant, surface water is relatively scarce, and flooding occurs frequently. Soil erosion and rocky desertification are among the major ecological and environmental challenges in the region.

The climate is predominantly subtropical monsoon, with abundant annual precipitation ranging from 900 to 1200 mm. Precipitation is spatially heterogeneous, with higher amounts in the east and lower amounts in the west. The mean annual temperature is approximately 14 °C, the annual sunshine duration is about 1700 h, and relative humidity exceeds 70%. The region supports diverse vegetation types and abundant forest resources. Land cover is mainly composed of forestland, shrubland, grassland, and cropland (Figure 1b).

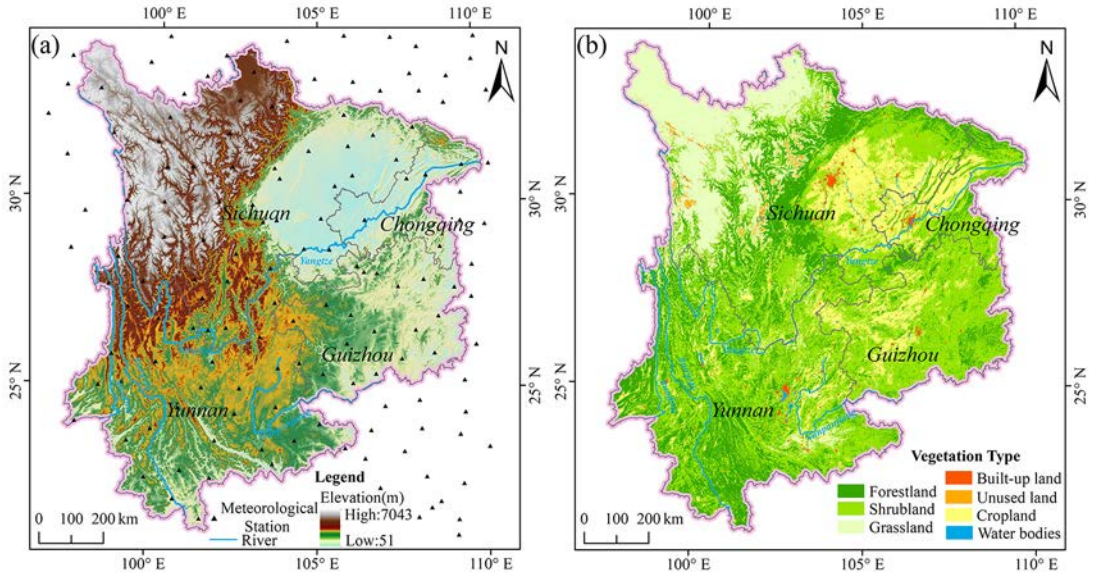


Figure 1. Geographic location of Southwest China (a) and land-use distribution in 2019 (b).

2.2. Data Sources and Preprocessing

Remote sensing data from 2001 to 2019 were obtained from the annual net primary productivity product (MOD17A3HGF v006) of the Moderate Resolution Imaging Spectroradiometer (MODIS), provided by the National Aeronautics and Space

Administration (NASA), with a spatial resolution of 500 m (https://ladsweb.modaps.eosdis.nasa.gov/).

Meteorological data were obtained from the National Meteorological Data Center of China (http://data.cma.cn/). Daily observations from 147 meteorological stations located in Southwest China and adjacent regions during 2001–2019 were collected, including temperature (tem), precipitation (pre), relative humidity (rhu), and sunshine duration (ssd) (Figure 1a). After evaluating the accuracy of the interpolated datasets and considering the strong influence of elevation on temperature, the thin-plate spline method (Hijmans et al., 2005; Zhu et al., 2019) was used to interpolate temperature data, with elevation included as a covariate. Precipitation, sunshine duration, and relative humidity were interpolated using the Kriging method. The spatial resolution of all interpolated meteorological datasets was standardized to 500 m.

Land-use data were derived from the MCD12Q1 product based on the International Geosphere–Biosphere Programme (IGBP) classification scheme and provided by NASA (https://ladsweb.modaps.eosdis.nasa.gov/), with a spatial resolution of 500 m. Land cover in the study area was classified into forestland, shrubland, cropland, grassland, built-up land, water bodies, and unused land. Because transitions involving water bodies and unused land were limited, they were not included in the subsequent analysis (Figure 1b).

The karst boundary used in this study was obtained from the National Earth System Science Data Center of China (http://www.geodata.cn/index.html) (Figure 2a). Data on rocky desertification control areas were acquired from the Global Change Research Data Publishing & Repository (https://www.geodoi.ac.cn/WebEn/Default.aspx). Digital elevation model (DEM) data were derived from the SRTM DEM UTM product, with a spatial resolution of 90 m, and were obtained from the Geospatial Data Cloud (http://www.gscloud.cn/).

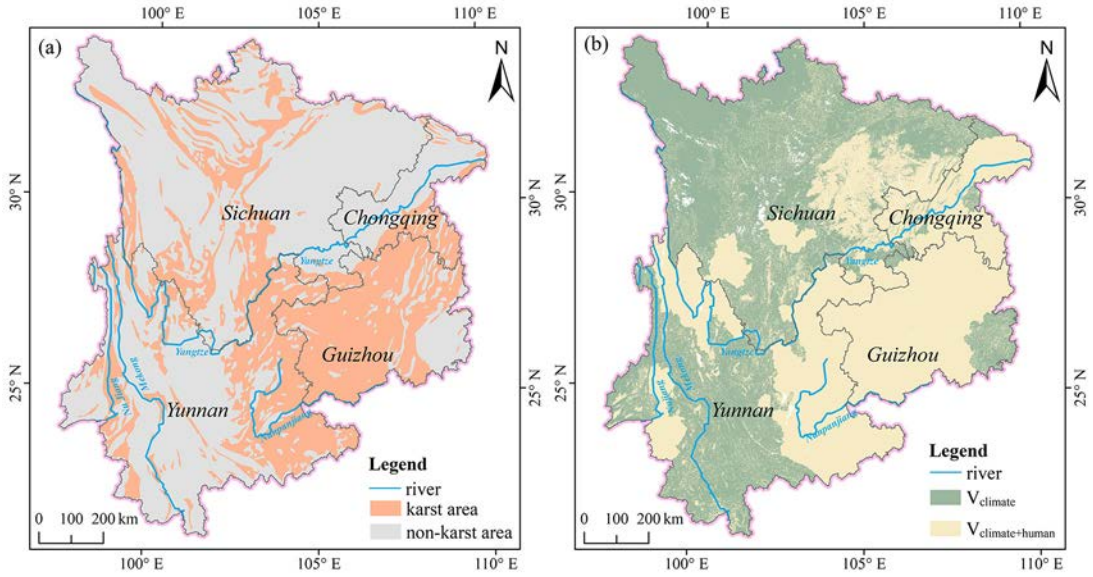


Figure 2. Distribution of karst areas (a) and distribution of $V_{climate}$ and $V_{climate+human}$ areas (b).

2.3. Methods

2.3.1. Trend Analysis

This study employed linear regression analysis to examine the spatiotemporal trends of NPP in Southwest China from 2001 to 2019. The calculation formula is as follows:

$$\theta_{slope} = \frac{n \times \sum_{i=1}^{n}(i \times NPP_i) - \sum_{i=1}^{n} i \sum_{i=1}^{n} NPP_i}{n \times \sum_{i=1}^{n} i^2 - \left(\sum_{i=1}^{n} i\right)^2} \quad (1)$$

Where, n represents the number of years in the time series (2001–2019, i.e., n=19); NPP_i is the NPP value for the i-th year; θ_{slope} denotes the interannual change rate for a given pixel. A positive slope indicates an increase in NPP over time, whereas a negative slope indicates a decrease. To assess the statistical significance of the trends, t-tests were conducted. Trends with P<0.01 were considered statistically significant. Based on the significance test results, the trends were categorized into four types: significant increase ($\theta_{slope} > 0$, $P < 0.01$), non-significant increase ($\theta_{slope} > 0$, $P > 0.01$), non-significant decrease ($\theta_{slope} < 0$, P>0.01), and significant decrease ($\theta_{slope} < 0$, $P < 0.01$).

2.3.2. Comprehensive NPP Changes in Land-Use Transition Areas

To characterize the overall changes in vegetation carbon sequestration capacity in

areas undergoing land-use transitions, land-use data from 2001 and 2019 were used to construct a land-use transition matrix. Based on the land-use transition matrix, the difference between the NPP after a given land-use type transitioned to other land-use types and the original NPP of the corresponding transition areas was calculated during 2001–2019. This difference represents the comprehensive NPP change in each land-use transition area. The calculation is expressed as follows:

$$\Delta NPP_{total} = NPP_{out} - NPP_{former} \quad (2)$$

Where, ΔNPP_{total} represents the comprehensive NPP change in areas undergoing transitions from a specific land-use type, including the combined effects of direct land-use transition, climatic fluctuations (e.g., temperature and precipitation), CO_2 fertilization effects, and other changes in environmental conditions. NPP_{out} represents the total NPP of areas after the transition from the original land-use type to other land-use types, and NPP_{former} represents the original total NPP of the corresponding transition areas before land-use transition. The quantitative contributions of climatic factors and human activities (including land-use transitions) to NPP changes are further separated using the partial derivative model described in Section 2.3.3.

2.3.3. Contribution analysis

In most studies that quantitatively separate the effects of climate and human activities, areas of natural vegetation are generally assumed to be jointly influenced by both factors. However, natural vegetation is often distributed in remote regions far from human settlements, where anthropogenic disturbances may be minimal. Consequently, this assumption may overestimate the effects of human activities on vegetation in sparsely populated or uninhabited areas (Ma et al., 2023).

To further quantify the contributions of climate and human activities, we conducted a two-step analysis. First, the study area was divided into areas with relatively low direct human disturbance and primarily influenced by climatic change and areas jointly influenced by climate change and human activities, denoted as $V_{climate}$ and $V_{climate+human}$, respectively, using land-use data and data on rocky desertification

control areas (Ge et al., 2021). The specific classification criteria were as follows. Cropland, built-up land, rocky desertification control areas, and areas experiencing land-use transitions were classified as $V_{climate+human}$ because they are frequently affected by human activities; an area meeting any one of these criteria was assigned to this category. After excluding the above areas, the remaining vegetated areas were classified as $V_{climate}$, which mainly consisted of natural vegetation, including forestland, shrubland, and grassland, with no land-use transitions during the study period. Unused land and water bodies were excluded from the analysis.

In terms of spatial distribution (Figure 2b), $V_{climate}$ had a mean elevation of approximately 2521 m, with forestland and shrubland accounting for approximately 70% of its total area. These areas were mainly distributed in sparsely populated regions, such as the western Sichuan Plateau and the Ailao Mountains in Yunnan. In contrast, $V_{climate+human}$ had a mean elevation of approximately 1493 m and was characterized by frequent human activities, with cropland and built-up land accounting for approximately 25% of the area. These areas were mainly distributed across the Sichuan Basin, Guizhou Province, and Chongqing Municipality.

Second, based on the above zoning results, partial derivative analysis was used to quantify the respective contributions of climatic factors and human activities to NPP changes (Wu et al., 2020). The calculation formula is as follows:

$$\begin{aligned}\frac{dNPP}{dt} &= \frac{\partial NPP}{\partial tem}\times\frac{dtem}{dt}+\frac{\partial NPP}{\partial pre}\times\frac{dpre}{dt}+\frac{\partial NPP}{\partial rhu}\times\frac{drhu}{dt}+\frac{\partial NPP}{\partial ssd}\times\frac{dssd}{dt}+UF \\ &= C(tem)+C(pre)+C(rhu)+C(ssd)+UF\end{aligned} \quad (3)$$

In the formula, $\frac{dNPP}{dt}$ represents the linear trend of *NPP* with time *t*, that is, the change trend of NPP. *Tem*, *pre*, *rhu*, and *ssd* represent the temperature, precipitation, relative humidity, and sunshine duration, respectively. *C*(*tem*), *C*(*pre*), *C*(*rhu*), and C(*ssd*) were the contributions of temperature, precipitation, relative humidity, and sunshine duration to the annual variation of NPP, respectively. UF represents the residual between NPP and the four climatic factors considered above, indicating the contributions of other factors, including anthropogenic factors (e.g., cultivation, carbon emissions, afforestation, and ecological restoration projects) and natural factors (e.g.,

geological hazards). In this study, UF was treated as a methodological approximation, assuming that this residual was primarily associated with human activities. $\frac{dtem}{dt}$, $\frac{dpre}{dt}$, $\frac{drhu}{dt}$, $\frac{dssd}{dt}$ represent the trends of each climatic factor with time. $\frac{\partial NPP}{\partial tem}$, $\frac{\partial NPP}{\partial pre}$, $\frac{\partial NPP}{\partial rhu}$ and $\frac{\partial NPP}{\partial ssd}$ respectively represent the partial derivatives of each climatic factor with respect to NPP. Each partial derivative was calculated while holding the other three factors constant, thereby quantifying the contribution of the target factor to NPP variation. The calculation formula is as follows:

$$R_{xy,zf\lambda} = \frac{R_{xy,zf} - R_{x\lambda,zf} \times R_{y\lambda,zf}}{\sqrt{(1 - R_{x\lambda,zf}^2) \times (1 - R_{y\lambda,zf}^2)}} \quad (4)$$

In the formula, $R_{xy,zf\lambda}$ representsthe partial correlation coefficient between x and y by eliminating the influence of z, f, and λ factors. $R_{xy,zf}$, $R_{x\lambda,zf}$, and $R_{y\lambda,zf}$ have similar definitions. The t-test was employed to determine the significance of the correlation between the two variables. The sign of the contribution indicates the direction of the corresponding effect on NPP. A positive effect signifies that the influencing factor promotes an increase in NPP, while a negative effect indicates that the influencing factor inhibits the increase in NPP.

2.3.4. Driving Force Analysis

Based on the results of trend analysis and contribution analysis, the following zoning criteria were applied to identify the dominant spatial driving patterns of climate and human activities on NPP changes.

Table 1. Classification criteria for NPP driving-force zones.

Slope	Climate	Human activities	Type
Slope>0	>0	>0	NPP increase driven by the combined effects of climate and human activities
	>0	<=0	NPP increase driven by climate
	<=0	>0	NPP increase driven by human activities
	<=0	<=0	Other factors
Slope<0	>=0	>=0	Other factors
	>=0	<0	NPP decrease driven by human activities
	<0	>=0	NPP decrease driven by climate
	<0	<0	NPP decrease driven by the combined effects of climate and human activities

3. Results

3.1. Spatiotemporal Characteristics of Vegetation NPP

From 2001 to 2019, the mean vegetation NPP in Southwest China was 736.84 $gC \cdot m^{-2}$, exhibiting a fluctuating increasing trend at a rate of 3.35 $gC \cdot m^{-2} \cdot yr^{-1}$ (Figure 3a). The lowest NPP value occurred in 2004 (682.35 $gC \cdot m^{-2}$), whereas the highest value was recorded in 2019 (770.38 $gC \cdot m^{-2}$). Notably, NPP reached local minima in 2004, 2010, and 2012. Spatially, the multi-year mean NPP ranged from 38.38 to 1945.97 $gC \cdot m^{-2}$. High-NPP areas were mainly distributed in southern Yunnan, where the dominant land-cover types were forestland and shrubland, whereas low-NPP areas were primarily concentrated in the Sichuan Basin and the western Sichuan Plateau, where cropland and natural grassland were the dominant land-cover types, respectively (Figure 4a). Overall, NPP increased across 77.00% of the study area, including 29.01% with a significant increase and 47.99% with a non-significant increase (Figure 4b; Table 2). In contrast, NPP showed a decreasing trend across 23.00% of the study area, of which only 2.20% exhibited a significant decrease.

NPP dynamics differed markedly between the karst and non-karst areas. The mean NPP in karst areas (780.27 $gC \cdot m^{-2}$) was higher than that in non-karst areas (710.79 $gC \cdot m^{-2}$), and the annual increase rate was also slightly higher in karst areas than in non-karst areas (3.42 vs. 3.31 $gC \cdot m^{-2} \cdot yr^{-1}$), indicating a relatively faster increase in vegetation productivity in karst areas during the study period (Figures 3b,c). The magnitude of interannual NPP variability was greater in karst areas than in non-karst areas. In karst areas, the minimum and maximum values occurred in 2004 (726.81 $gC \cdot m^{-2}$) and 2019 (826.69 $gC \cdot m^{-2}$), respectively, whereas in non-karst areas, they occurred in 2001 (664.89 $gC \cdot m^{-2}$) and 2019 (751.85 $gC \cdot m^{-2}$), respectively. In addition, the proportion of karst areas showing a significant increase in NPP (26.59%) was lower than that in non-karst areas (30.45%), whereas the proportions showing a non-significant increase (52.17%) and a significant decrease (2.64%) were both higher than those in non-karst areas (45.49% and 1.94%, respectively) (Table 2).

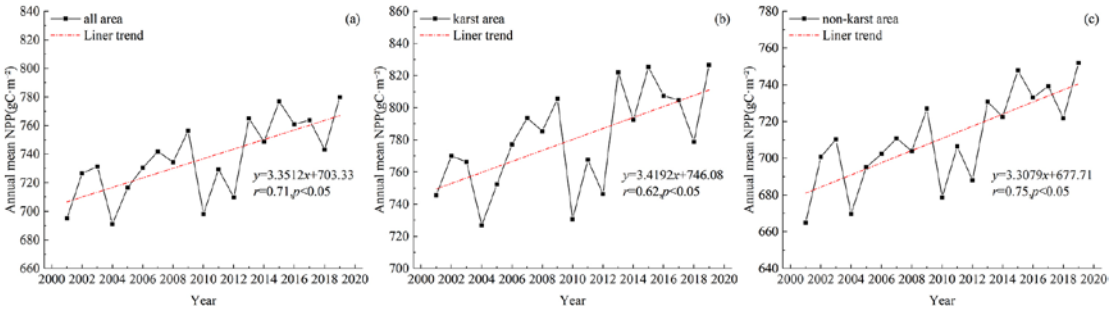


Figure 3. Interannual variations in vegetation NPP in the study area (a), karst areas (b), and non-karst areas (c) during 2001–2019.

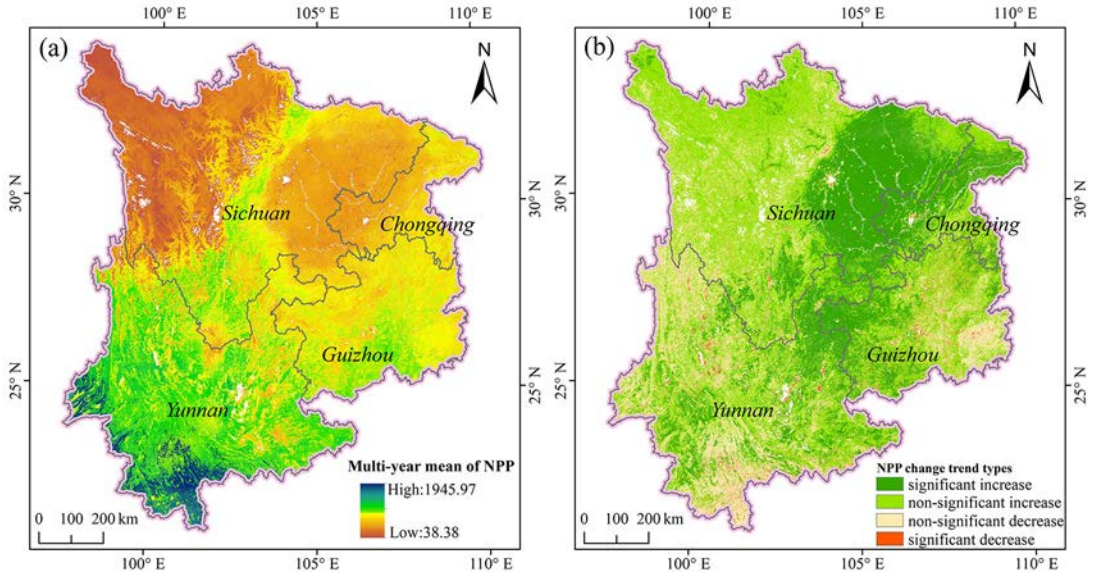


Figure 4. Spatial distribution of the multi-year mean vegetation NPP (a) and the spatial distribution of NPP trend categories (b).

Table 2. Area proportions of different NPP trend categories in the study area, karst areas, and non-karst areas (%).

	Significant increase	Non-significant increase	Non-significant decrease	significant decrease
All areas	29.01%	47.99%	20.80%	2.20%
Karst	26.59%	52.17%	18.60%	2.64%
Non-karst	30.45%	45.49%	22.13%	1.94%

3.2. NPP Changes in Land-Use Transition Areas

Land use is strongly influenced by human activities and represents an important factor affecting NPP dynamics (Sun et al., 2021). From 2001 to 2019, the total area undergoing land-use transitions was 69,254.25 km² in the karst areas, accounting for 16.41% of their total area, compared with 94,940.93 km² in the non-karst areas, accounting for 13.45% (Figure 5). These results indicate a higher degree of land-use

dynamics in the karst areas. The overall patterns of land-use transitions were broadly consistent between the karst and non-karst areas. Among the land-use types transitioning out, shrubland had the largest transition area, with 36,529.17 km² in the karst areas and 51,776.46 km² in the non-karst areas; of these transition areas, 87.70% and 86.18%, respectively, transitioned to forestland (Figure 5). Cropland had the second-largest transition area, with 11,989.55 km² in the karst areas and 18,409.97 km² in the non-karst areas, of which 95.01% and 90.39%, respectively, transitioned to shrubland. Among the land-use types transitioning in, forestland had the largest transition area, with 32,290.95 km² in the karst areas and 44,985.54 km² in the non-karst areas, approximately 99% of which originated from shrubland (Figures 5a,b). Built-up land had the smallest transition area, with 320.09 km² in the karst areas, mainly originating from shrubland and cropland, and 1,983.42 km² in the non-karst areas, mainly originating from cropland and shrubland (Figure 5).

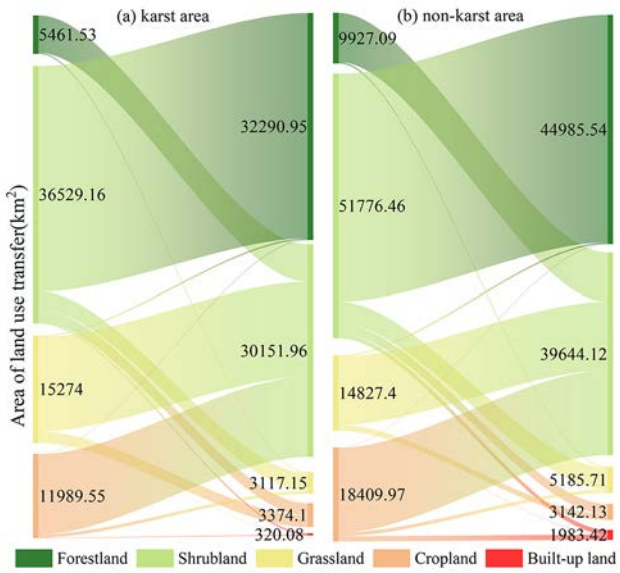


Figure 5. Sankey diagrams illustrating land-use transitions in karst and non-karst areas of Southwest China during 2001–2019.

Based on the land-use transition matrix, the overall NPP changes from 2001 to 2019 were calculated for areas transitioning into and out of different land-use types. As shown in Figure 6, the areas transitioning to forestland showed the largest NPP increases among all transition categories, with increases of 342.27 gC·m^{-2} in karst areas and 355.15 gC·m^{-2} in non-karst areas. Among these areas, those transitioning

from cropland to forestland showed the largest NPP increases, with increases of 135.57 $gC \cdot m^{-2}$ in karst areas and 188.58 $gC \cdot m^{-2}$ in non-karst areas (Figures 6a,c). Comparisons between karst and non-karst areas revealed different NPP changes across the same land-use transition categories. In areas transitioning from forestland to shrubland, NPP increased by 7.32 $gC \cdot m^{-2}$ in karst areas but decreased by 12.24 $gC \cdot m^{-2}$ in non-karst areas (Figures 6a,d). In areas transitioning from shrubland to cropland, NPP decreased by 76.95 $gC \cdot m^{-2}$ in karst areas but increased by 66.37 $gC \cdot m^{-2}$ in non-karst areas (Figures 6b,c). In addition, the NPP increases in areas transitioning from grassland to forestland and from grassland to shrubland were greater in karst areas (120.09 and 112.64 $gC \cdot m^{-2}$, respectively) than in non-karst areas (90.71 and 65.65 $gC \cdot m^{-2}$, respectively). In terms of NPP decreases, areas transitioning out of forestland showed a greater NPP decrease in non-karst areas (111.61 $gC \cdot m^{-2}$), whereas areas transitioning to built-up land showed a greater NPP decrease in karst areas (363.55 $gC \cdot m^{-2}$) (Figures 6b,d).

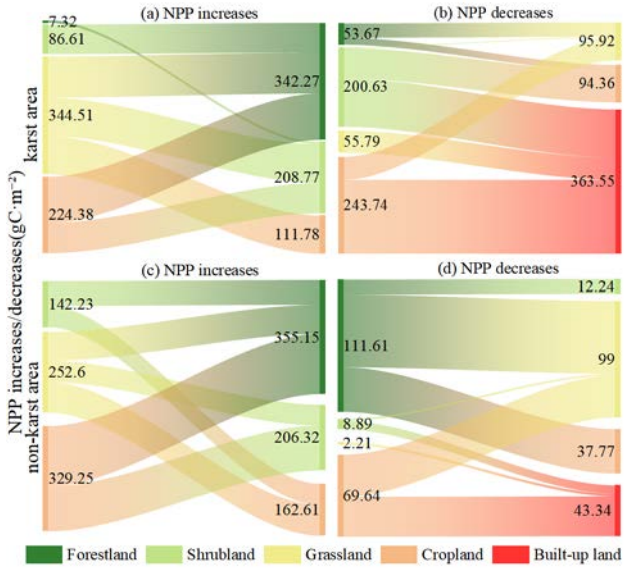


Figure 6. Sankey diagrams showing the overall increases and decreases in NPP in land-use transition areas. (a) NPP increases in karst areas; (b) NPP decreases in karst areas; (c) NPP increases in non-karst areas; and (d) NPP decreases in non-karst areas.

3.3. Attribution Analysis of NPP Changes

3.3.1. Contributions of Climate and Human Activities to NPP Changes

From 2001 to 2019, climatic variables showed varying interannual fluctuations in both the karst and non-karst areas of the study region. Precipitation in the karst areas

showed an overall non-significant increasing trend at a rate of 30.00 mm·10a^{-1} (P > 0.05), which was higher than that in the non-karst areas (23.12 mm·10a^{-1}) (Figure 7a). Relative humidity exhibited an overall non-significant increasing trend in the karst areas at a rate of 2.56%·10a^{-1} (P > 0.05), whereas it showed a non-significant decreasing trend in the non-karst areas at a rate of 0.49%·10a^{-1} (P > 0.05) (Figure 7b). Sunshine duration exhibited an overall non-significant decreasing trend in the karst areas at a rate of 14.18 h·10a^{-1} (P > 0.05), whereas it showed a non-significant increasing trend in the non-karst areas at a rate of 5.89 h·10a^{-1} (P > 0.05) (Figure 7c). Temperature increased significantly in both areas, with rates of 0.24 °C·10a^{-1} in the karst areas and 0.27 °C·10a^{-1} in the non-karst areas (P < 0.05) (Figure 7d). Overall, temperature and relative humidity were higher in the karst areas than in the non-karst areas, whereas sunshine duration showed the opposite pattern.

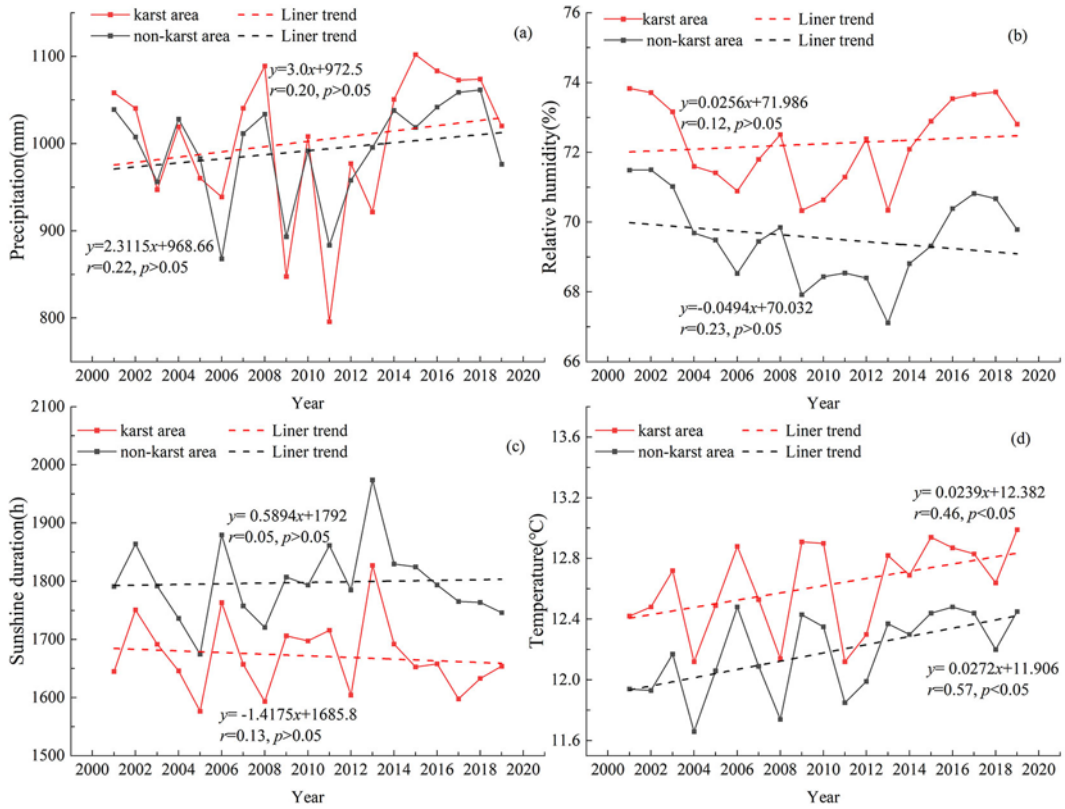


Figure 7. Interannual variations in climatic factors in Southwest China during 2001–2019. (a) Precipitation; (b) Relative humidity; (c) Sunshine duration; and (d) Temperature.

Based on the contribution analysis, the total climatic contribution (i.e., the sum of the climatic contribution separated from $V_{climate+human}$ areas and that from $V_{climate}$ areas)

and the human activity contribution estimated using the residual proxy (i.e., the residual term UF separated from $V_{climate+human}$ areas and used as an approximate measure of human activity contribution) were obtained. The climatic contribution and the estimated human activity contribution to NPP changes are summarized in Table 3 and Figures 8–10. The estimated human activity contribution was the dominant contribution to NPP changes in the study area, with a mean contribution of 3.09 $gC \cdot m^{-2} \cdot yr^{-1}$, compared with 1.03 $gC \cdot m^{-2} \cdot yr^{-1}$ for the climatic contribution. Regional comparisons showed that the estimated human activity contribution was higher in the karst areas (3.245 $gC \cdot m^{-2} \cdot yr^{-1}$) than in the non-karst areas (2.92 $gC \cdot m^{-2} \cdot yr^{-1}$), while the proportion of karst areas showing negative effects was lower than that of non-karst areas (24.80% vs. 29.21%). In contrast, the climatic contribution was lower in the karst areas (0.594 $gC \cdot m^{-2} \cdot yr^{-1}$) than in the non-karst areas (1.289 $gC \cdot m^{-2} \cdot yr^{-1}$), with a higher proportion of negative climatic effects in the karst areas (39.89% vs. 33.88%). Among the climatic factors, precipitation made the largest contribution to NPP. Its contribution was lower in the karst areas (0.349 $gC \cdot m^{-2} \cdot yr^{-1}$) than in the non-karst areas (0.958 $gC \cdot m^{-2} \cdot yr^{-1}$), while the proportion of negative effects was higher in the karst areas (43.22% vs. 31.95%). Sunshine duration ranked second, contributing 0.24 $gC \cdot m^{-2} \cdot yr^{-1}$ and 0.338 $gC \cdot m^{-2} \cdot yr^{-1}$ in the karst and non-karst areas, respectively. Temperature made only a small contribution to NPP changes (approximately 0.006–0.007 $gC \cdot m^{-2} \cdot yr^{-1}$), although its positive effects were widely distributed, accounting for approximately 76.43% of the study area. Relative humidity contributed negatively to NPP in the non-karst areas (−0.006 $gC \cdot m^{-2} \cdot yr^{-1}$) but positively in the karst areas (0.003 $gC \cdot m^{-2} \cdot yr^{-1}$); the proportion of negative effects of relative humidity was also higher in the non-karst areas than in the karst areas (54.09% vs. 43.83%). Overall, NPP changes in the karst areas were more strongly associated with the estimated contribution of human activities, whereas climatic constraints were stronger and the direct positive effect of precipitation was more limited. In contrast, the non-karst areas showed a greater climatic contribution and more pronounced positive effects of precipitation, while NPP was also subject to negative effects associated with relative humidity and human activities.

Table 3. Mean climatic contribution and estimated mean human activity contribution ($gC \cdot m^{-2} \cdot yr^{-1}$).

Region	Temperature	precipitation	sunshine duration	Relative humidity	climate	Human activities
All Areas	0.006	0.729	0.301	-0.003	1.030	3.090
Karst	0.007	0.349	0.240	0.003	0.594	3.245
Non-Karst	0.006	0.958	0.338	-0.006	1.289	2.920

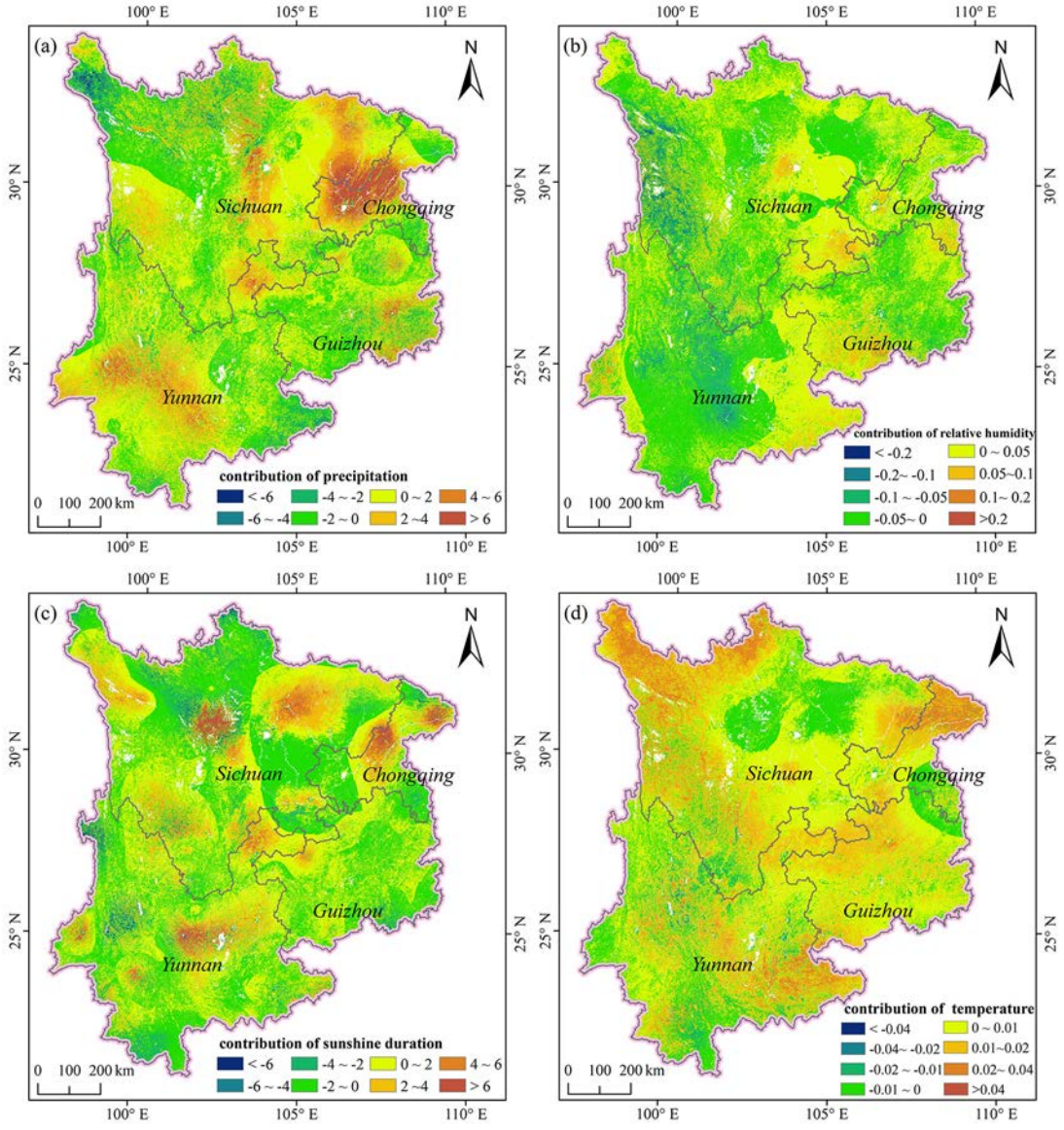


Figure 8. Spatial distribution of the contributions of (a) precipitation, (b) relative humidity, (c) sunshine duration, and (d) temperature to NPP changes. (Positive values indicate positive effects on NPP, whereas negative values indicate negative effects on NPP.)

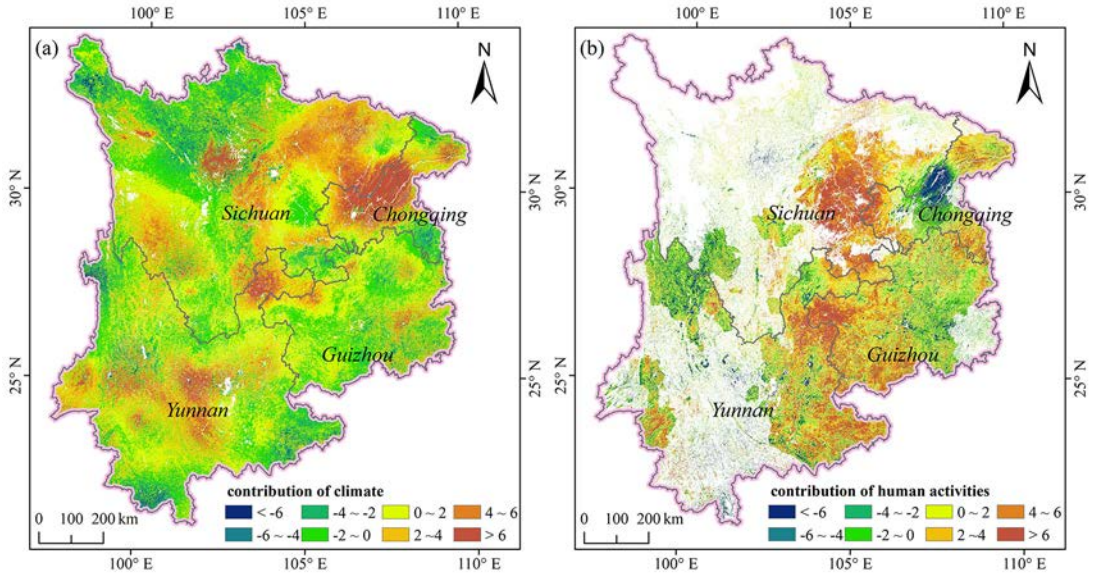


Figure 9. Spatial distribution of (a) climatic contributions and (b) estimated human activity contributions to NPP changes. Positive contributions indicate positive effects that promote NPP increases, whereas negative contributions indicate negative effects that inhibit NPP increases.

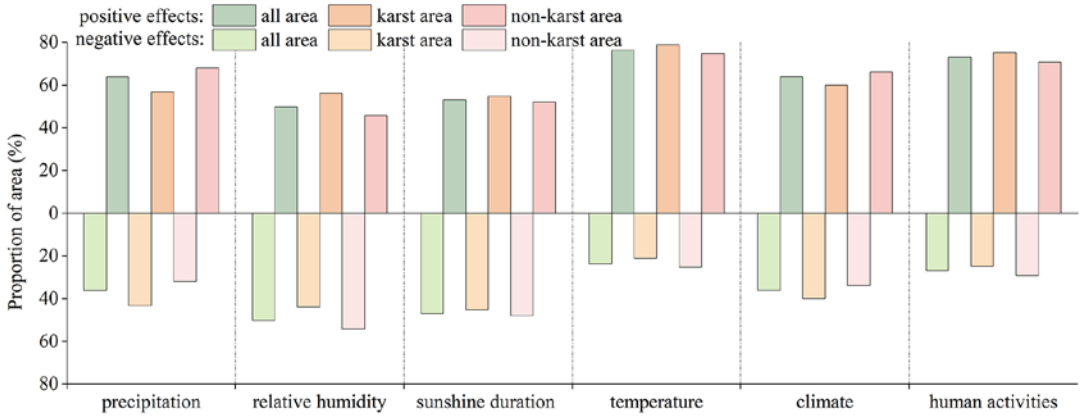


Figure 10. Area proportions of positive and negative effects of climatic factors and human activities on NPP changes. (Positive effects indicate enhancement of NPP, whereas negative effects indicate suppression of NPP.)

3.3.2. Driving Force Analysis

The aforementioned contribution analysis quantified the contributions of individual factors to NPP changes but was insufficient to fully reveal the dominant driving patterns and their spatial differences between karst and non-karst areas. To further identify the dominant drivers of NPP changes under different geological backgrounds, we integrated NPP trends, climatic contributions, and the estimated human activity contribution to classify and analyze the driving forces of NPP changes.

Overall, NPP increases were mainly attributable to positive climatic driving (27.12% of the study area, with a rate of change of 4.58 $gC \cdot m^{-2} \cdot yr^{-1}$) and the combined driving effects of climate and human activities (25.02% of the study area, with a rate of change of 7.73 $gC \cdot m^{-2} \cdot yr^{-1}$). Meanwhile, human activities exhibited a stronger driving effect on NPP changes than climate, as indicated by their higher rate of change (5.30 vs. 4.58 $gC \cdot m^{-2} \cdot yr^{-1}$) (Figure 12). Regional comparisons revealed that in karst areas, areas with NPP increases driven by human activities and the combined effects of climate and human activities were particularly extensive (Figure 11 and Figure 12). The area proportion of NPP increase driven by human activities accounted for 21.43% of the area (change rate: 5.40 $gC \cdot m^{-2} \cdot yr^{-1}$), mainly distributed in eastern Yunnan, central Guizhou, and Chongqing. In contrast, the area proportion driven by the combined effects of climate and human activities was higher, at 32.57% (change rate: 6.87 $gC \cdot m^{-2} \cdot yr^{-1}$), mainly distributed in northern Yunnan and southwestern Guizhou. By comparison, the area proportion of NPP increase driven by climate in karst areas accounted for only 17.24% (change rate: 3.57 $gC \cdot m^{-2} \cdot yr^{-1}$), with a scattered distribution. In non-karst areas, climate-driven NPP increase was more prominent, covering 33.03% of the area (change rate: 4.90 $gC \cdot m^{-2} \cdot yr^{-1}$), mainly distributed in central Chongqing, western Sichuan, and central Yunnan. This was higher than the area proportion driven by human activities (7.27%; change rate: 5.13 $gC \cdot m^{-2} \cdot yr^{-1}$) (Figures 11, 12). Regarding NPP decreasing trends, the area proportion of NPP decrease driven by the combined effects of climate and human activities was the smallest in both karst and non-karst areas, whereas the corresponding change rates were the largest (-6.03 $gC \cdot m^{-2} \cdot yr^{-1}$ and -6.07 $gC \cdot m^{-2} \cdot yr^{-1}$, respectively), indicating that the combined effects were associated with greater NPP declines than either single factor (Figure 12). In summary, the magnitude of NPP changes was more strongly influenced by the combined effects of climate and human activities. NPP changes in karst areas were primarily driven by human activities, with climate playing a secondary role, whereas those in non-karst areas were primarily climate-driven, with human activities playing a secondary role. These differences suggest distinct NPP response patterns under contrasting geological backgrounds and combinations of climatic and anthropogenic

factors.

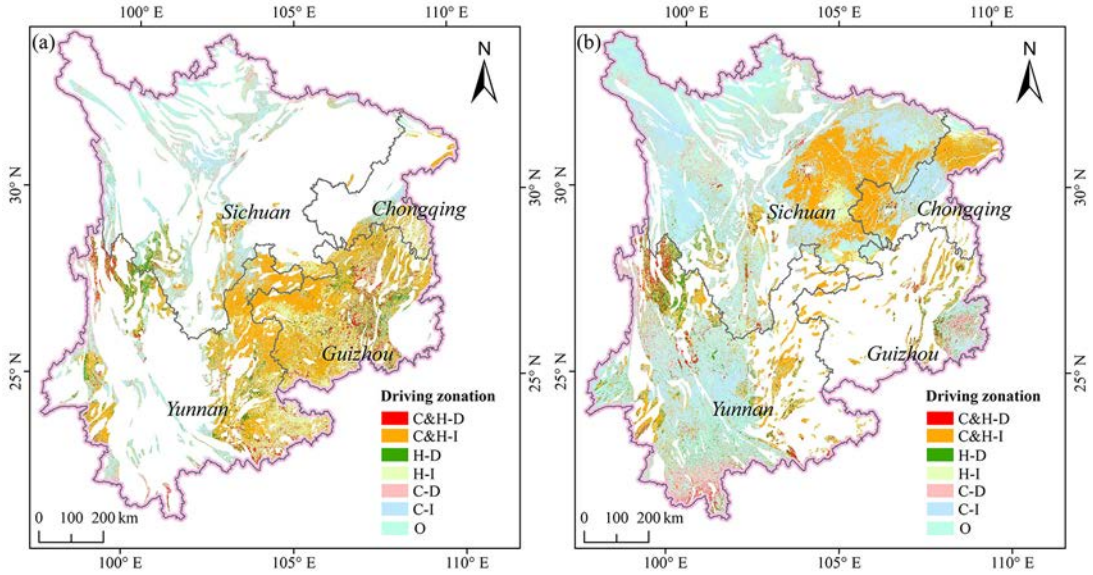


Figure 11. Spatial distribution of vegetation NPP change driven by climate and human activities in karst (a) and non-karst (b) areas. (C&H-I, NPP increase driven by the combined effects of climate and human activities; C&H-D, NPP decrease driven by the combined effects of climate and human activities; H-I, NPP increase driven by human activities; H-D, NPP decrease driven by human activities; C-I, NPP increase driven by climate; C-D, NPP decrease driven by climate; O, other factors.)

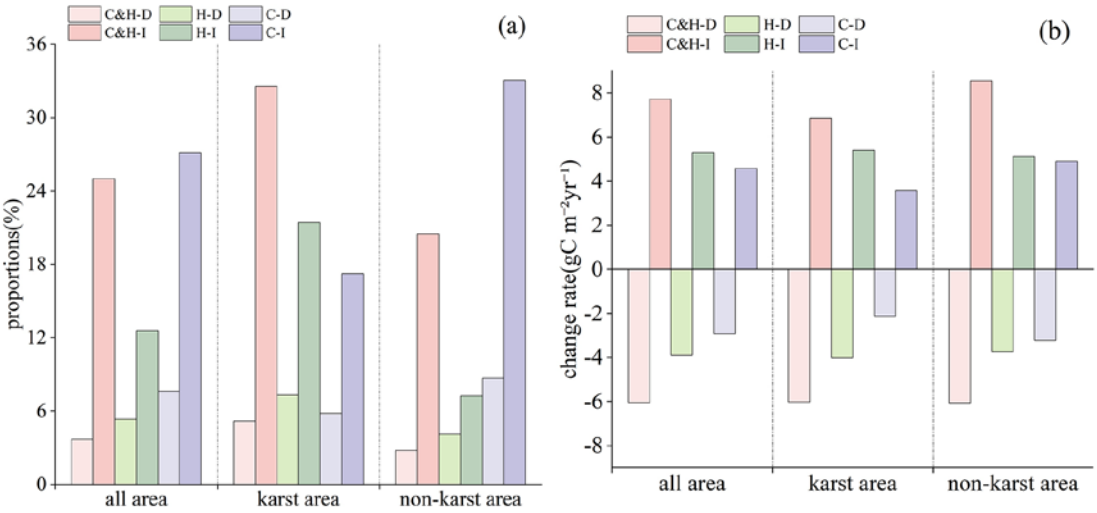


Figure 12. Area proportions (a) of NPP changes driven by climate and human activities and the corresponding NPP change rates (b) in each region. (C&H-I, NPP increase driven by the combined effects of climate and human activities; C&H-D, NPP decrease driven by the combined effects of climate and human activities; H-I, NPP increase driven by human activities; H-D, NPP decrease driven by human activities; C-I, NPP increase driven by climate; C-D, NPP decrease driven by climate; O, other factors; The change rate represents the magnitude of NPP variation in the corresponding regions, while the area proportion reflects the spatial extent of each driving category.)

4. Discussion

4.1. Differences between Karst and Non-Karst Areas

This study revealed the spatiotemporal dynamics of vegetation NPP in Southwest China from 2001 to 2019 and examined its responses to climate and human activities. The results demonstrated that both the spatiotemporal patterns and driving mechanisms of NPP varied with geological background.

Among the climatic factors, NPP in the karst areas exhibited a weaker response to climatic variability, which was closely associated with the distinctive geological characteristics of these areas, particularly the limited utilization of precipitation by vegetation (Wu et al., 2020; Zhang et al., 2023). Although precipitation increased at a higher rate in the karst areas than in the non-karst areas, its availability to vegetation is constrained by the shallow soils and extensive rock exposure associated with carbonate bedrock. These conditions enhance runoff and soil erosion (Liu et al., 2024; Shuai et al., 2025; Liu et al., 2026). Moreover, the distinctive dual-layer hydrological structure of karst areas promotes rapid water infiltration through fissures and conduits, thereby reducing water-retention capacity and vegetation water availability (Liu et al., 2016; Luo et al., 2024). In contrast, the non-karst areas generally have deeper soil layers and greater water-storage capacity, allowing precipitation to provide a more effective water supply for vegetation growth. The concurrent increases in temperature and sunshine duration (Figure 7) may also favor photosynthesis. Consequently, climate change exerts a more pronounced positive effect on NPP in the non-karst areas. In addition, relative humidity exhibited opposite contributions between the two areas. In the non-karst areas, increases in temperature, precipitation, and sunshine duration coincided with a non-significant decline in relative humidity (Figure 7), which may have reduced water-use efficiency and thereby contributed negatively to NPP (Lu et al., 2025). In contrast, because water availability is already constrained by karst leakage, increasing relative humidity may alleviate the pressure for stomatal closure in karst areas and thus contribute positively to NPP (Song et al., 2021; Shuai et al., 2025). The karst areas of Southwest China are characterized by frequent cloud and fog conditions

and have lower annual sunshine duration than the non-karst areas (Figure 7c), which may constrain vegetation photosynthesis and consequently result in a lower contribution of sunshine duration to NPP in the karst areas. NPP in the study area reached local minima in 2004, 2010, and 2012, which may have been associated with regional extreme climatic events (Xiao et al., 2024).

Land use is strongly influenced by human activities and is an important factor affecting NPP changes. From 2001 to 2019, land-use transitions in both the karst and non-karst areas were dominated by transitions to forestland, which were closely associated with long-term ecological restoration projects in Southwest China. By 2019, the total afforestation area in Southwest China had reached 21.7738 million ha, including 15.2130 million ha of artificial afforestation, 4.9389 million ha of forest protection through mountain closure, and 3.6332 million ha of cropland-to-forestland restoration, resulting in an expansion of vegetation cover. Our results showed that NPP increased most strongly in areas transitioning to forestland, with cropland-to-forestland transitions showing the most pronounced NPP increase. This finding suggests that favorable land-use transitions may contribute to regional NPP enhancement and, indirectly, indicates the potential of ecological restoration projects such as cropland-to-forestland conversion to enhance NPP (Zhang et al., 2023; Du et al., 2024). However, the observed NPP changes represent integrated changes resulting from multiple environmental and anthropogenic factors; therefore, the causal contribution of specific ecological restoration projects cannot be isolated based on the present analysis alone.

However, differences in geological background between karst and non-karst areas were associated with contrasting NPP responses under the same land-use transition types. In karst areas, NPP increased in areas transitioning from forestland to shrubland, whereas NPP decreased in corresponding areas in non-karst areas. This pattern is consistent with the ecological fragility and rocky desertification characteristics of karst ecosystems. Shrublands may exhibit higher vegetation productivity because shrubs generally have greater tolerance to extreme drought and saline–alkali conditions (Ma et al., 2023; Xiao et al., 2024), whereas in non-karst areas, more favorable soil conditions

generally support higher productivity in forestlands than in shrublands. Similarly, NPP decreased in areas transitioning from shrubland to cropland in karst areas but increased in corresponding areas in non-karst areas. This difference may mainly reflect variations in site conditions and cropland management practices between the two areas (Wu et al., 2026). In karst areas, croplands are often distributed on gentle slopes with shallow soils and high rock exposure. Areas undergoing shrubland-to-cropland transitions generally experience severe soil erosion and low nutrient availability, limiting crop productivity (Luo et al., 2024). In contrast, areas undergoing shrubland-to-cropland transitions in non-karst areas generally have more fertile soils and better agricultural management practices, which may promote increases in crop NPP.

The results of both the contribution and driving-force analyses showed that human activities and the combined effects of climate and human activities accounted for 54% of the areas showing increasing NPP in the karst areas, whereas NPP increases driven solely by climate were less extensive. This suggests that human activities played a relatively greater role in NPP increases in the karst areas. Under climatic constraints on vegetation productivity in karst areas, positive anthropogenic interventions, such as cropland-to-forestland restoration and rocky desertification control, may therefore serve as important compensatory drivers for enhancing NPP. Zhou et al. (2025) similarly reported that forestland restoration was the primary source of vegetation NPP changes in the karst areas of Southwest China, with cropland identified as the main land-use source driving forestland restoration, supporting the findings of this study. The karst areas are also key areas for the implementation of ecological restoration projects, where anthropogenic interventions may contribute to vegetation improvement (Hong et al., 2021). This may partly explain why the rate of NPP increase was higher in the karst areas than in the non-karst areas. Compared with non-karst areas, karst ecosystems generally exhibit lower survival rates of planted trees, weaker resistance of vegetation productivity to external disturbances, lower ecosystem stability, poorer restoration quality, and reduced carbon sequestration capacity (Sun et al., 2013; Liu et al., 2024; Luo et al., 2024). These characteristics help explain why the proportion of areas with significant NPP increases is lower in karst areas and why the

risk of localized degradation remains slightly higher. In addition, NPP changes in some areas could not be adequately explained by the factors considered above and may have been influenced by other factors, such as wind speed, CO_2 concentration, and grazing. Further investigation is therefore needed to clarify their potential effects.

These findings suggest that vegetation carbon enhancement in karst areas should not simply replicate the tree-planting-oriented restoration model commonly adopted in non-karst areas. Instead, restoration strategies should prioritize vegetation types with stronger environmental adaptability, such as shrubland, and incorporate complementary measures, including water conservation and soil improvement. Such diversified approaches may help achieve synergies between carbon sequestration and ecosystem stability.

Table 4. Cumulative Afforestation Area in Southwest China During 2001–2019 ($\times 10^4$ ha).

Region	Total Afforestation Area	Planted Forests	Natural Forest Regeneration	Cropland Conversion to Forest
Sichuan	627.8588	381.3094	155.2641	98.0976
Chongqing	326.1136	201.6263	90.6769	73.3052
Yunnan	763.3434	618.8134	97.3241	106.6278
Guizhou	460.0702	319.5507	150.6247	85.2842
Total	2177.386	1521.2998	493.8898	363.3148

4.2. Uncertainties and limitations

The zoning scheme adopted in this study involves several sources of uncertainty. Human activities that do not alter land-use types, such as mountain closure measures for forest protection, grazing, and recreational activities in forest areas, were assigned to the $V_{climate}$ areas. Therefore, these areas cannot be regarded as completely climate-dominated zones, which may introduce uncertainty into the quantitative attribution results. In addition, the residual term may incorporate the effects of natural hazards, such as debris flows and landslides. Because this study approximately assumed that the residual was primarily driven by human activities, this simplification may introduce potential biases into the attribution results.

The 500 m spatial resolution of the remote-sensing data may also limit the ability to capture small-scale changes in land-use types, and individual pixels may contain

multiple vegetation types. Moreover, this study considered only temperature, precipitation, sunshine duration, and relative humidity as climatic factors affecting NPP in Southwest China. Potential influences of disturbances such as fire and CO_2 concentration were not incorporated, and lagged vegetation responses to climate change were not considered. Furthermore, land-use changes and ecological restoration projects cannot fully represent the breadth of human activities. Other factors, including population density, the secondary industry, and grazing, may also affect NPP. These factors should be incorporated into future analyses to further improve the attribution of NPP dynamics.

5. Conclusions

Based on remote sensing data, this study investigated the spatiotemporal variation characteristics of vegetation NPP in Southwest China from 2001 to 2019. By integrating land-use and meteorological data, the study systematically analyzed the spatiotemporal evolution of vegetation productivity in karst and non-karst areas and their differential responses to climate and human activities. The main conclusions of this study are as follows:

(1) From 2001 to 2019, NPP in Southwest China exhibited an overall increasing trend. Although NPP increased more rapidly in the karst areas, NPP stability was relatively lower and localized risks of decline were higher. Therefore, greater attention should be given to the precise identification and targeted management of patches showing declining NPP trends in karst areas.

(2) Vegetation carbon sequestration capacity under the same land-use transitions differed between karst and non-karst areas. Compared with non-karst areas, the NPP increase in areas transitioning from cropland to forestland was relatively limited in karst areas, potentially owing to shallow soils and low nutrient availability. In contrast, NPP increases in areas transitioning from grassland to forestland or shrubland were greater in karst areas. For some of the same land-use transitions, opposite NPP changes were observed between karst and non-karst. These findings suggest that tree-planting-oriented restoration strategies should not be simply applied to karst areas.

In karst areas, cropland-to-forestland restoration should be accompanied by soil improvement measures, while grassland-to-forestland or grassland-to-shrubland transitions may provide alternative pathways.

(3) The contribution analysis showed that the estimated human activity contribution based on the residual proxy was the main contributor to NPP increases, although clear spatial differences in its contribution were observed. NPP increases in the karst areas were more strongly associated with human activities, whereas the contribution of climate was relatively limited. In contrast, NPP in the non-karst areas was more sensitive to climatic variability than that in the karst areas, with precipitation making a particularly pronounced positive contribution.

(4) Overall, the combined effects of climate and human activities were strongly associated with the magnitude of NPP changes. In the context of ecological engineering projects, such as rocky desertification control, NPP changes in karst areas were predominantly associated with human activities and combined climate–human activity effects, whereas the contribution of climatic drivers was relatively weaker, potentially constrained by the regional geological background. In non-karst areas, where soil and water conditions were generally more favorable, NPP changes were more strongly associated with climatic drivers. These contrasting patterns highlight the need for differentiated ecological management strategies tailored to different geological backgrounds.

Conflict of Interests: The author declares no conflict of interest.

Funding

This research was funded by the Science and Technology Project of Chongqing Geological Survey Bureau (Grant No: DKJ-2024-NJD-B-005) and the Project of Chongqing Municipal Bureau of Planning and Natural Resources (Grant No: CQS22C00432).

Reference

Du C C., Bai X Y., Li Y B., Tan Q., Zhao C W., Luo G J., Wang J F., Wu L H., Li C J.,

Li J H., Xie Y H., Ran C., Zhang S., Xiong L., Yuang X D., Liao J J., Dai L., Long M K., Li Z L., Xue Y Y., Zhang X Y., Luo Q., Shen X Q., Yang S., Li M H., 2024, The restoration of karst rocky desertification has enhanced the carbon sequestration capacity of the ecosystem in southern China. Global and Planetary Change 243:104602. https://doi.org/10.1016/j.gloplacha.2024.104602.

Chen Y Z., Chen L Y., Cheng Y., Ju W M., Chen H., Ruan H H., 2020, Afforestation promotes the enhancement of forest LAI and NPP in China. Forest Ecology and Management 462:117990. https://doi.org/10.1016/j.foreco.2020.117990.

Erb K H., Fetzel T., Plutzar C., Kastner T., Lauk C., Mayer A., Niedertscheifer M., Koner C., Haberl H., 2016, Biomass turnover time in terrestrial ecosystems halved by land use. Nature Geoscience 9:674-678. https://doi.org/10.1038/NGEO2782.

Ewuketu L., Hoga JA., Cao M., Zhang W F., Yang X F., Hu Y H., 2020, Precipitation influences on the net primary productivity of a tropical seasonal rainforest in Southwest China: A 9-year case study. Forest Ecology and Management 467:118153. https://doi.org/10.1016/j.foreco.2020.118153.

Ge W Y., Deng L Q., Wang F., Han J Q., 2021, Quantifying the contributions of human activities and climate change to vegetation net primary productivity dynamics in China from 2001 to 2016. Science of the Total Environment 773:145648. https://doi.org/10.1016/j.scitotenv.2021.145648.

Guan X B., Shen H F., Li X H., Gan W G., Zhang L P., 2019, A long-term and comprehensive assessment of the urbanization-induced impacts on vegetation net primary productivity. Science of the Total Environment 669:342-352. https://doi.org/10.1016/j.scitotenv.2019.02.361.

Guo B., Han B., Yang F., Chen S T., Liu Y., Yang W., 2020, Determining the contributions of climate change and human activities to the vegetation NPP dynamics in the Qinghai-Tibet Plateau, China, from 2000 to 2015. Environmental Monitoring and Assessment 192:663. https://doi.org/10.1007/s10661-020-08606-6.

Hijmans RJ., Cameron SE., Parra JL., Jones PG., Jarvis A., 2005, Very high resolution interpolated climate surfaces for global land areas. International Journal of Climatology 25(15):1965–1978. https://doi.org/10.1002/joc.1276.

Hong X X., Huang Y., Sun T., 2021, Spatiotemporal evolution of vegetation net primary productivity in the karst region of Southwest China from 2001 to 2018. Acta Ecologica Sinica 41(24):9836-9846. https://doi.org/10.5846/stxb202009122381.

Lu B Y., Yao H., Zhu L S., Chen Z L., 2025, Comprehensive response assessment of water use efficiency to climate change in ecologically fragile karst areas. Environmental and Sustainability Indicators 27:100834. https://doi.org/10.1016/j.indic.2025.100834.

Liu C Y., Dong X f., Liu Y Y., 2015, Changes of NPP and their relationship to climate factors based on the transformation of different scales in Gansu, China. Catena 125:190-199. https://doi.org/10.1016/j.catena.2014.10.027.

Luo D., Zhou Z F., Zhang L., Chen Q., Huang D H., Feng Q., Wu T Y., Wu L., 2024, Evolution and driver analysis of forest carbon stocks in karst mountainous areas

of southwest China in the context of rocky desertification management. Catena 246:108335. https://doi.org/10.1016/j.catena.2024.108335.

Liu M X., Xu X L., Wang D B., Sun AY., Wang K L., 2016, Karst catchments exhibited higher degradation stress from climate change than the non-karst catchments in southwest China: An ecohydrological perspective. Journal of Hydrology 535:173-180. https://doi.org/10.1016/j.jhydrol.2016.01.033.

Liu W Q., Zhu D Y., Zhao Y S., Han Y R., Tan J Y., Yin J Y., 2026, Comparison of the centennial spatiotemporal evolution of rainfall erosivity in the top three global karst regions. Journal of Hydrology 664:134528. https://doi.org/10.1016/j.jhydrol.2025.134528.

Liu H X., Zhang A B., Liu C., Zhao Y L., Zhao A Z., Wang D L., 2021, Analysis of the time-lag effects of climate factors on grassland productivity in Inner Mongolia. Global Ecology and Conservation 30:e01751 . https://doi.org/10.1016/j.gecco.2021.e01751.

Liu H Y., Mi Z R., Lin L., Wang Y H., Zhang Z H., Zhang F W., Wang H., Liu L L., Zhu B., Cao G M., Zhao X Q., Sanders N J., T.Classen A., Reich P B., 2018, Shifting plant species composition in response to climate change stabilizes grassland primary production. Sustainbility Science 115:4051. https://doi.org/10.1073/pnas.1700299114.

Liu Y Y., Lian J J., Chen H S., 2024, Assessment of the restoration potential for ecological sustainability in the Xijiang River basin, Southwest China: A comparative analysis of karst and non-karst areas. Science of the Total Environment 912:168929, https://doi.org/10.1016/j.scitotenv.2023.168929.

Lv Y., Zhang L., Yan H M., Ren X L., Wang J B., Niu Z E.,Gu F X., He H L., 2018, Spatial and temporal patterns of changing vegetation and the influence of environmental factors in the karst region of Southwest China. Acta Ecologica Sinica 38(24):8774-8786. https://doi.org/10.5846/stxb201807251593.

Ma B X., Jing J L., Liu B., Wang Y F., He H C., 2023, Assessing the contribution of human activities and climate change to the dynamics of NPP in ecologically fragile regions. Global Ecology and Conservation 42:e02393, https://doi.org/10.1016/j.gecco.2023.e02393.

Nemani R R., Keeling C D., Hashimoto H., Jolly W M., Piper S C., Tucker C J., Myneni R B., Running S W., 2003, Climate-driven increases in global terrestrial net primary production from 1982 to 1999. Science 300:1560-1563. https://doi.org/10.1126/science.1082750.

Prestele R., Arneth A., Bondeau A., Noblet-Ducoudre N D., Pugh T A.M., Sitch S., Stehfest E., Verburg P H., 2017, Current challenges of implementing anthropogenic land-use and land-cover change in models contributing to climate change assessments. Earth System Dynamics 8(2):369-386. https://doi.org/10.5194/esd-8-369-2017.

Shuai N., Hu Y C., Bai Y P., Wang J., Guo Z L., 2025, Impact of drought on vegetation carbon fixation in karst areas: A study of south China's continuous greening. Journal of Environmental Management 395:127826. https://doi.org/10.1016/j.jenvman.2025.127826.

Song X M., Bai P., Ding J P., Li J M., 2021, Effect of vapor pressure deficit on growth

and water status in muskmelon and cucumber. Plant Science 303:110755. https://doi.org/10.1016/j.plantsci.2020.110755.

Sun D L., Zhang J Y., Zhou Q W., 2013, Study on repair technology of degraded vegetation ecosystems in Karst regions. Guangdong Agricultiral Sciences (3): 135-138. https://doi:10.16768/j.issn.1004-874x.2013.03.016.

Sun Z J., Xie S Y., 2021, Spatiotemporal variation in vegetation net primary productivity and factor detection in Yunnan Province based on geodetector. Chinese Jounal of Ecology 40(12):3836-3848. https://doi.org/10.13292/j.1000-4890.202111.033.

Taelman S E., Schaubroeck T., De M S., Boone L., Dewulf J., 2016, Accounting for land use in life cycle assessment: the value of NPP as a proxy indicator to assess land use impacts on ecosystems. Science of the Total Environment 550:143-156. https://doi.org/10.1016/j.scitotenv.2016.01.055.

Teng M J., Zeng L X., Hu W J., Wang P C., Yan Z G.,He W., Zhang Y., Huang Z L., Xiao W F., 2020, The impacts of climate changes and human activities on net primary productivity vary across an ecotone zone in Northwest China. Science of the Total Environment 714:136691. https://doi.org/10.1016/j.scitotenv.2020.136691.

Wang Y., Sun J., Liu M., Zeng T., Tsunekawa A., Mubaarak A A., Zhou H K., 2019, Precipitation-use efficiency may explain net primary productivity allocation under different precipitation conditions across global grassland ecosystems. Global Ecology and Conservation 20:e00713. https://doi.org/10.1016/j.gecco.2019.e00713.

Wang Y H., Dai E F., Wu C S., 2021, Spatiotemporal heterogeneity of net primary productivity and response to climate change in the mountain regions of southwest China. Ecological Indicators 132:108273. https://doi.org/10.1016/j.ecolind.2021.108273.

Wu L H., Wang S J., Bai X Y., Tian Y C., Luo G J., Wang J F., Li Q., Chen F., Deng Y H., Yang Y J., Hu Z Y., 2020, Climate change weakens the positive effect of human activities on karst vegetation productivity restoration in southern China. Ecological Indicators 115:106392. https://doi.org/10.1016/j.ecolind.2020.106392.

Wu L Z., Ma X F., Dou X., Zhu J T., Zhao C Y., 2021, Impacts of climate change on vegetation phenology and net primary productivity in arid Central Asia. Science of the Total Environment 796:149055. https://doi.org/10.1016/j.scitotenv.2021.149055.

Wu S H., Zhou S L., Chen D X., Wei Z Q., Dai L., Li X G., 2014, Determining the contributions of urbanisation and climate change to NPP variations over the last decade in the Yangtze River Delta, China. Science of the Total Environment 472:397-406. https://doi.org/10.1016/j.scitotenv.2013.10.128.

Wu Y., Tian C H., Li T., Li M Y., 2026, Forest unrealized potential productivity in karst regions – A case study in Guizhou Province, China. Forest Ecology and Management 612:123728. https://doi.org/10.1016/j.foreco.2026.123728.

Xiao L Y., Wu X Q., Zhao S., Zhou J X., 2024, Memory effects of vegetation after extreme weather events under various geological conditions in a typical karst watershed in southwestern China. Agricultural and Forest Meteorology

345:109840. https://doi.org/10.1016/j.agrformet.2023.109840.
Yan Y C., Wu C J., Wen Y Y., 2021, Determining the impacts of climate change and urban expansion on net primary productivity using the spatio-temporal fusion of remote sensing data. Ecological Indicators 127:107737. https://doi.org/10.1016/j.ecolind.2021.107737.
Yang H F., Zhong X N., Deng S Q., Xu H., 2021, Assessment of the impact of LUCC on NPP and its influencing factors in the Yangtze River basin, China. Catena 206:105542. https://doi.org/10.1016/j.catena.2021.105542.
Zhang W., Xi M Z., Liu H D., Zheng H., 2023, Low sensitivity of net primary productivity to climatic factors in three karst provinces in southwest China from 1981 to 2019. Ecological Indicators 153:110465. https://doi.org/10.1016/j.ecolind.2023.110465.
Zhang Y J., Wu J X., Pan Y., Zhang X Z., 2022, Human appropriation of net primary production: A review. Proggress in Geography 41(2):341-350, https://doi.org/10.18306/dlkxjz.2022.02.013.
Zhao P., Wang D J., He S T., Lan H J., Chen W L., Qi Y C., 2020, Driving forces of NPP change in debris flow prone area: A case study of a typical region in SW China. Ecological Indicators 119:106811. https://doi.org/10.1016/j.ecolind.2020.106811.
Zheng K., Wei J Z., Pei J Y., Cheng H., Zhang X L., Huang F Q., Li F M., Ye J S., 2019, Impacts of climate change and human activities on grassland vegetation variation in the Chinese Loess Plateau. Science of the Total Environ 660:236-244. https://doi.org/10.1016/j.scitotenv.2019.01.022.
Zhong J., Liu J F., Jiao L M., Lian X H., Xu Z H., Zhou Z Z., 2021, Assessing the comprehensive impacts of different urbanization processes on vegetation net primary productivity in Wuhan, China, from 1990 to 2020. Sustainable Cities and Society. https://doi.org/10.1016/j.scs.2021.103295.
Zhou K S., Du J., Shen X., Pu G J., Zhang D D., Dang X N., 2021, Spatiotemporal changes of vegetation net primary productivity in the Qiangtang National Nature Reserve under climate change. Chinese Journal of Agrometeorology 42(8):627-641. https://doi.org/10.3969/j.issn.1000-6362.2021.08.001.
Zhou Z F., Zhu M., Wu X P., Liu R P., Wang J L., Wan J X., Zheng J J., 2025, Quantifying the impact pathways and driving mechanisms of increased forest CS: A comparative study case from typical karst ecologically fragile and non-karst areas. Ecological Engineering 213:107544. https://doi.org/10.1016/j.ecoleng.2025.107544.
Zhu W B., Zhang X D., Zhang J J., Zhu L Q., 2019, A comprehensive analysis of phenological changes in forest vegetation of the Funiu Mountains, China. Journal of Geographical Sciences 29(1):131-145. https://doi.org/10.1007/s11442-019-1588-z.